Chinese Chemical Letters 36 (2025) 109994

Contents lists available at ScienceDirect

Chinese Chemical Letters

journal homepage: www.elsevier.com/locate/cclet

One-pot accessing of *meso*–aryl heptamethine indocyanine NIR fluorophores and potential application in developing dye-antibody conjugate for imaging tumor

Mengxing Liu, Jing Liu*, Hongxing Zhang, Jianan Tao, Peiwen Fan, Xin Lv, Wei Guo*

School of Chemistry and Chemical Engineering, Shanxi University, Taiyuan 030006, China

ARTICLE INFO

Article history:
Received 20 February 2024
Revised 6 May 2024
Accepted 10 May 2024
Available online 11 May 2024

Keywords:
Heptamethine indocyanines
Aryl substituents
Aromatic lithium reagents
Protein labeling
Imaging tumor

ABSTRACT

In this work, we put forward a new and universal approach, *i.e.*, cyanine ketone method, for fabricating *meso*–aryl heptamethine indocyanines, which is so simple that the treatment of the easy-to-get cyanine ketones with various aromatic lithium (ArLi), followed by acidification, could straightforwardly give rise to the products in one-pot way. Importantly, due to the strong nucleophilicity of ArLi, a series of bulky hydrophilic aromatic groups can be facilely integrated into the *meso*–position of heptamethine indocyanines, not only effectively inhibiting the undesired dye self-aggregation but also largely improving the water-solubility. Using one of anti-aggregation *meso*–aryl heptamethine indocyanines, we fabricated a dye-antibody conjugate for *in vivo* imaging tumor in a mouse model and achieved a high tumor-to-normal tissue ratio. The work laid a chemical foundation for constructing various *meso*–aryl heptamethine indocyanines, facilitating the advanced imaging and therapeutic applications in future.

Fluorescence technique, as a nonionizing radiation method, is one of the most powerful cellular biology tools to study biomedical phenomena, by which imaging and tracing of various biological species and dynamic biological events within living cells or body could be achieved [1-5]. Over the past 30 years, fluorescence techniques have been revolutionarily advanced, typically including confocal laser scanning microscopy (CLSM), two-photon laser scanning fluorescence microscopy (TPLSM), single molecule localization microscopy (SMLM), structure illumination microscopy (SIM), and imaging-guided surgery (IGS) system [6-9]. Meanwhile, these advances also pose a great challenge on developing more robust fluorescent dyes to match the increasing requirements, especially those with absorption and emission wavelengths in the near-infrared (NIR) range (700–900 nm), a favorable spectral window due to the reduced background signal, enhanced tissue penetration, minimum photodamage to biological samples, and invisibility to eyes that ensures the look of surgical field undisturbed [10,11].

Among various fluorescent dyes, cyanine dyes, since their first synthesis in 1856, have become the extremely valuable fluorophores in chemistry, biology, and medical diagnosis [12]. Within this family, heptamethine indocyanine dyes (Cy7), containing seven conjugated carbon atoms in the polyene linker, are particularly attractive due to their NIR absorption and emission wavelengths (commonly > 750 nm) and exceptionally large molar extinction coefficients (commonly $> 2.0 \times 10^5$ L mol^{-1} cm^{-1}). The most typical heptamethine indocyanine is indocyanine green (**ICG**) (Scheme 1A), the only Food and Drug Administration (FDA)-approved NIR optical marker for clinical uses [13]. However, **ICG** is known for its poor stability and moderate fluorescent properties; moreover, strong self-aggregation due to its hydrophobic polyene core, heavily binding to serum proteins arising from its unbalanced surface charges, and obvious background fluorescence due to the high uptake in liver and gastrointestinal tract also compromise its imaging application [14,15]. More disadvantageous for **ICG** is the absence of a single reactive site in its molecular skeleton, which greatly limits its derivatization for improving its targetability for various diagnosis applications. Fortunately, the dilemma was broken since the development of the conjugatable *meso*–chloro–substituted heptamethine indocyanines **Cl-Cy7** (Scheme 1B) [16,17], whose post-synthetic modification *via* the reactive *meso* C-Cl bond promptly leaded to a variety of *meso*–position-functionalized heptamethine indocyanines, either as fluorescent probes to image biological species [11], or as NIR photocaging groups to prompt the spatial and temporal control of drug delivery [18,19], or as phototherapeutic agents to ablate tumors [20-23].

From pre-clinical or clinical perspective, a **Cl-Cy7**-derived representive example is polyanionic **CW800** (IRDye CW800®)

* Corresponding authors.
E-mail addresses: liujing4203@sxu.edu.cn (J. Liu), guow@sxu.edu.cn (W. Guo).

https://doi.org/10.1016/j.cclet.2024.109994
1001-8417/

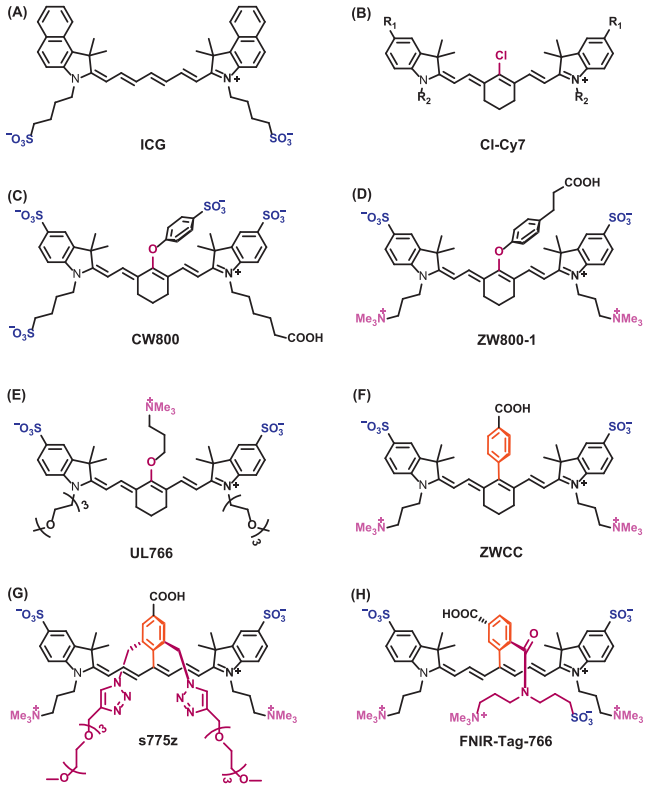

Scheme 1. (A–H) Chemical structures of the representative heptamethine cyanine fluorophores reported previously.

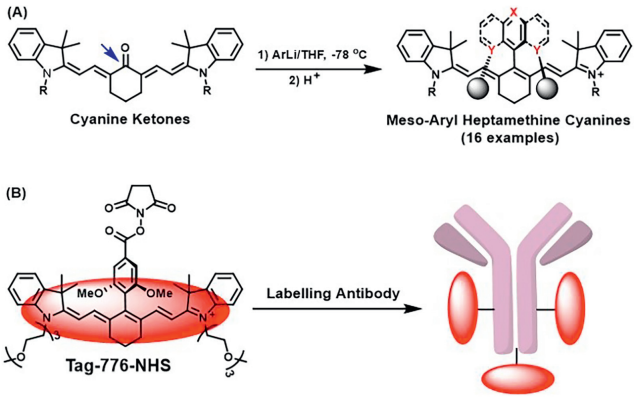

Scheme 2. (A) Cyanine ketone method for fabricating various *meso*–aryl heptamethine indocyanines. X refers to C or N atom, Y to C or O atom, and spherical body to the sterically shielded arms. (B) Application in developing anti-aggregation labeling agent **Tag-776-NHS** to label antibody for *in vivo* imaging tumor.

(Scheme 1C), a commercially available *meso* C–O aryl heptamethine indocyanine that has been developed into NIR fluorescent probes for real-time visualization of operating field, allowing accurate identification and resection of tumors [24,25]. However, the polyanionic structure (four -SO_3^- groups) makes the dye or its protein conjugates to suffer from the non-optimal pharmacokinetics and obvious background fluorescence due to the non-specific staining with off-target proteins by electrostatic interaction [26-28]. To overcome the limit, the charge-balanced zwitterionic structures, such as **ZW800–1** (Scheme 1D), were subsequently exploited, which largely decreases non-specific staining and efficiently promotes renal clearance, thus substantially increasing the tumor-to-background ratio [29-31]. However, both **CW800** and **ZW800–1** contain a chemically unstable *meso* C-O aryl bond, which is easy to suffer from the attack of intracellularly rich thiols or amines to cause chemical degradation [32,33]. Soon afterwards, the issue was intelligently addressed by replacing the reactive *meso* C-O aryl bond with the more robust *meso* C-O alkyl bond *via* the electrophile-integrating Smiles rearrangement, as exemplified by **UL766** (Scheme 1E) [34,35]. However, due to the strong electron-donating ability of the *meso* C–O alkyl group, the electron-rich heptamethine indocyanines are susceptible to photobleaching caused by the simultaneously generated singlet oxygen [36]. Recognizing these shortcomings, the *meso*–aryl heptamethine indocyanines, featured with a more robust *meso* C–C bond and a less electron-donating *meso*–aryl group, subsequently aroused researchers' keen interest, as exemplified by **ZWCC** (Scheme 1F) [37-39]. Although improved significantly in chemo- and photostability, the series of dyes exhibited extensive self-aggregation in water, especially the nonfluorescent H-aggregation, due to their rigid hydrophobic cores [40,41], thus largely retarding their practical imaging application. As is known, dye self-aggregation is detrimental to protein labeling because it drives multiple self-aggregated dyes to covalently bind at proximal lysine positions on protein surface, partially quenching the fluorescence, influencing protein functions, and also promoting undesired protein aggregation [40-43]. Therefore, how to efficiently inhibit the self-aggregation of *meso*–aryl heptamethine indocyanines in water subsequently becomes a pressing issue. Recently, two sterically shielded *meso*–aryl heptamethine indocyanines **s775z** and **FNIR-Tag-766** (Schemes 1G and H) [44,45], along with their bioconjugates, were intelligently synthesized, both of which displayed strong anti-aggregation ability in water, indicating that the sterically shielding arm at the *ortho* positions of the *meso*–aryl substituent play a critical role in preventing self-aggregation. However, the synthesis of the two dyes is multi-step and technically demanding, which may hinder their uses in preclinical research. Thus, developing a simpler method to access the sterically shielded *meso*–aryl heptamethine indocyanines is urgently needed.

Generally, the *meso*–aryl heptamethine indocyanines could be prepared by way of the Pd-catalyzed Suzuki-Miyaura cross-coupling of **Cl-Cy7** and arylboronic acids or arylborate esters in aqueous solution [37-39,41,46-48], which was first reported in 2006 [39]. However, the method only works well in aqueous solution, thus being greatly confined to prepare those highly hydrophilic and cell membrane-impermeable ones; moreover, the method is hardly used to fabricate the sterically shielded *meso*–aryl heptamethine indocyanines presumably due to the Pd-catalyzed cross-coupling incompatible with the arylboronic acid or arylborate ester with the large steric groups at its *ortho*-positons. The other method is the direct condensation of a custom Schiff base with indolenine [49,50]. However, the method is only used to prepare *meso*–phenyl and *meso*–methyl heptamethine indocyanines to date, probably because of the difficult synthesis of the related Schiff base with the bulkyl Aryl substituent in its *meso*–position. Recently, by employing the ring opening reaction of Zincke salts [44,51] or PyBox [45] salts, two sterically shielded and anti-aggregation *meso*–aryl heptamethine indocyanines, *i.e.*, **s775z** and **FNIR-Tag-766** (Schemes 1G and H), were synthesized. However, as mentioned above, the two multi-step synthetic methods are technically demanding.

In this work, for the first time we put forward a simple and universal "cyanine ketone method" for fabricating the *meso*–aryl heptamethine indocyanine NIR fluorescent dyes (Scheme 2A). As seen, the treatment of the easy-to-get cyanine ketones with various aromatic lithium reagents (ArLi), followed by acidification, could directly give rise to *meso*–aryl heptamethine indocyanines in one-pot way. Importantly, thanks to the strong nucleophilicity of ArLi reagents, various bulky hydrophilic aromatic groups could easily

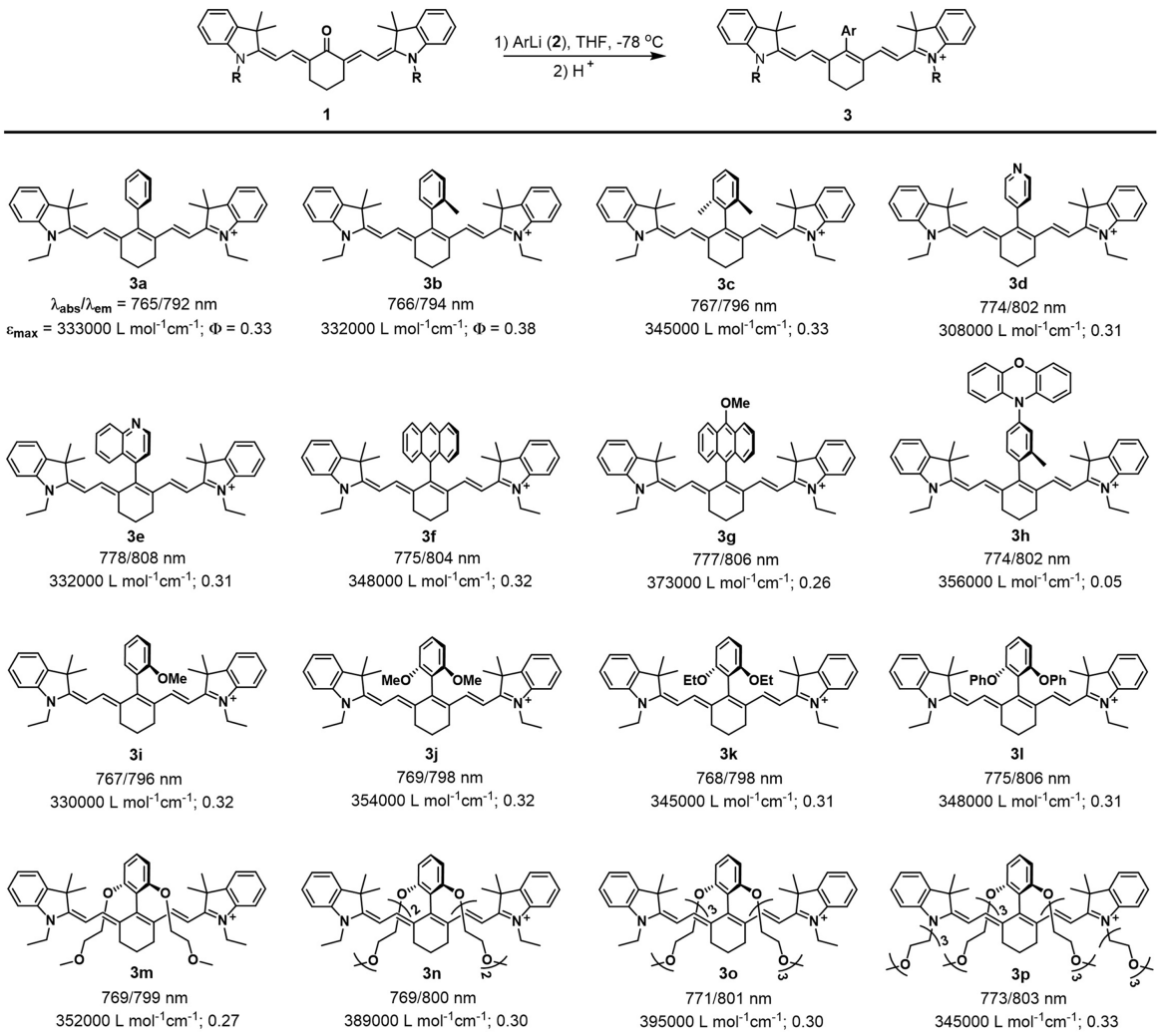

Fig. 1. Various *meso*–aryl heptamethine cyanine fluorophores synthesized by our one-pot cyanine ketone method in this work. Absorption maxima (λ_{abs}, nm)/emission maxima (λ_{em}, nm), molar extinction coefficients (ε, L mol^{-1} cm^{-1}), and fluorescence quantum yields [Φ, determined using Cy7 ($\Phi_f = 0.24$ in MeOH) as a reference] measured in CH_2Cl_2 were shown.

be integrated into the *meso*–position of heptamethine indocyanine skeletons, enabling the facile one-pot accessing of the sterically shielded and anti-aggregation *meso*–aryl heptamethine indocyanines. Using one of the anti-aggregation *meso*–aryl heptamethine indocyanines, we have successfully fabricated a PEGylated protein labeling agent **Tag-776-NHS** to label monoclonal antibody panitumumab for *in vivo* imaging tumor (Scheme 2B), and obtained a high tumor-to-normal (T/N) tissue ratio in a tumor-bearing mouse model.

Our design was inspired by the synthesis of *meso*–aryl rhodamine fluorophores that employed xanthones as the precursors [52-55]. We envisioned that the approach should also be amenable to the synthesis of *meso*–aryl heptamethine indocyanines, provided that cyanine ketone precursor **1** (Fig. 1) could be easily obtained. In fact, the compound was first synthesized in 1992 by the one-step reaction of **Cl-Cy7** with sodium acetate in *N*,*N*-dimethylformamide (DMF), showing absorption and emission maxima at 535 nm and 625 nm, respectively [56]. Upon protonation, it could be transformed into *meso*–hydroxyl cyanine with absorption and emission maxima at 710 nm and 730 nm, respectively [57-61]. The early work is the start point of our subsequent studies. According to the reported procedure [56], we first synthesized the simplest cyanine ketone **1a**, and then tested its reaction with phenyl lithium **2a** in THF at −78 °C. To our delight, the reaction, followed by acidification with aqueous 1 mol/L HCl, provided the *meso*–phenyl heptamethine indocyanine **3a** in 82.4% yield (Fig. 1). This result reveals that our *cyanine ketone method* should be feasible for fabricating various *meso*–aryl heptamethine indocyanines.

Encouraged by the above result, we subsequently tested the generality of our "cyanine ketone method". As expected, by the reaction of cyanine ketone **1a** with various aryl lithium reagents **2**, followed by acidification, a series of *meso*–aryl heptamethine indocyanines **3** with varied steric bulk in the *meso*–position could conveniently be synthesized, including *meso*–2-methylphenyl **3b**, *meso*–2,6-dimethylphenyl **3c**, *meso*–pyridin-4-yl **3d**, *meso*–quinolin-4-yl **3e**, *meso*–anthran-9-yl **3f**, *meso*–10-methoxyanthran-9-yl **3g**, and *meso*–4-(phenoxazin-10-yl)–2-methlyphenyl **3h** (Fig. 1). The chemical structures of the above compounds were confirmed by ^{1}H-nuclear magnetic resonance spectroscopy (NMR), ^{13}C NMR, and high-resolution mass spectrometry (HRMS) spectra (Supporting information). Notably, a main objective using the "cyanine ketone method" is to construct the water-soluble and sterically shielded *meso*–aryl heptamethine indocyanines to inhibit the dye self-aggregation in water for effective protein labeling. Actually, previous studies on **s775z** and **FNIR-Tag-766** (Schemes 1G and H) have indicated that the water-soluble and bulky sub-

stituents in the *ortho* positions of *meso*–aryl group play critical roles in improving water-solubility and preventing dye self-aggregation [44,45]. With the idea in mind, we further synthesized *meso*–2-methoxyphenyl **3i**, *meso*–2,6-dimethoxyphenyl **3j**, *meso*–2,6-diethoxyphenyl **3k**, and *meso*–2,6-diphenoxyphenyl **3l** through our "cyanine ketone method" (Fig. 1), and demonstrated that, among the series, *meso*–2,6-dimethoxyphenyl **3j** has the best water-solubility (octanol/water partition coefficient: Log*P* = 1.005) and the strongest anti-aggregation ability in phosphate buffer solution (PBS, 10 mmol/L, pH 7.4), as indicated by the exclusive monomer absorption band even in the high concentration of 40 μmol/L (Fig. S1 in Supporting information). By comparison, in the same condition, **ICG** and *meso*–2-methoxyphenyl **3i** showed obvious H-aggregation band, and *meso*–2,6-diethoxyphenyl **3k** and *meso*–2,6-diphenoxyphenyl **3l** had low and negligible water-solubility, respectively (Fig. S1), due to the more hydrophobic *meso*–2,6-diethoxyphenyl and *meso*–2,6-diphenoxyphenyl groups. To further improve the water solubility, we synthesized a series of PEGylated *meso*–aryl heptamethine indocyanines, including *meso*–2,6-di(ethylene glycol monomethyl ether)-substituted phenyl **3m**, *meso*–2,6-di(dipolyethylene glycol monomethyl ether)-substituted phenyl **3n**, and *meso*–2,6-di(tripolyethylene glycol monomethyl ether)-substituted phenyl **3o**, by our "cyanine ketone method" (Fig. 1), and demonstrated that the introduction of two ethylene glycol monomethyl ether or two polyethylene glycol (PEG) monomethyl ether chains in the 2,6-positions of the *meso*–aryl group greatly improved the water-solubility of these dyes, as indicated by the gradually decreased Log*P* values (Log*P*: 0.849 for **3m**, 0.431 for **3n**, and 0.403 for **3o**) when compared with that of *meso*–2,6-dimethoxyphenyl **3j** (Log*P* = 1.005); meanwhile, all of them exhibited the strong anti-aggregation ability in PBS due to the presence of two bulky sterically shielded arms in their *meso*–aryl group (Fig. S1). The story is not over yet, because it is still possible to replace the hydrophobic indolenine *N*-ethyl group with the water-soluble PEG_3 chain to further improve the water-solubility. Moving on, we synthesized a PEGylated cyanine ketone precusor **1b**, by which we obtained a fully PEGylated dye **3p** by our "cyanine ketone method" (Fig. 1). As expected, the molecule, featured with four PEG_3 chains in its molecular structure, showed the highest water-solubility (Log*P* = 0.092) among the series; moreover, no any self-aggregation was observed in PBS in the concentration range of 2–40 μmol/L (Fig. S1). The chemical structures of these dyes were also confirmed by ^{1}H NMR, ^{13}C NMR, and HRMS spectra (Supporting information).

The photophysical properties of **3a**–**3p** were evaluated in dichloromethane (CH_2Cl_2), acetonitrile (MeCN), and PBS (10 mmol/L, pH 7.4, containing 30% MeCN for ensuring all the dyes are soluble), respectively, and compared with a conventional heptamethine indocyanine **Cy7** (Table S1 in Supporting information). The absorption and emission spectra were shown in Figs. S2–S4 (Supporting information). As seen, these *meso*–aryl heptamethine indocyanines all show NIR absorption/emission wavelengths with maxima in the ranges of 757–778 nm/784–811 nm, respectively, longer than those of control dye **Cy7** due to the stronger electron-withdrawing property of *meso*–aryl groups than that of *meso*–H atom. The fluorescence quantum yields of these dyes (Φ: 0.26–0.41 in CH_2Cl_2; 0.18–0.32 in CH_3CN; 0.12–0.24 in PBS) are comparable or higher than those of control dye **Cy7**, except for **3h** (Φ: 0.05 in CH_2Cl_2; 0.07 in CH_3CN; 0.07 in PBS) whose strongly electron-donating phenoxazine group effectively quenches fluorescence *via* the photoinduced electron transfer (PeT). Noteworthily, these dyes all exhibit the considerably large molar extinction coefficients (ε: 2.00–3.95 × 10^5 L mol^{-1} cm^{-1}), higher than those of control dye **Cy7** (2.00–2.48 × 10^5 L mol^{-1} cm^{-1}) in the same solvent. As a result, their fluorescence brightnesses ($\varepsilon \times \Phi$), except for **3h**, are obviously higher than those of control dye **Cy7** with the maxima up to 126,000 L mol^{-1} cm^{-1} in CH_2Cl_2 (for **3b**) and 58,000 L mol^{-1} cm^{-1} in PBS (for **3a** and **3p**). In addition, all these *meso*–aryl heptamethine indocyanines show similar absorption and emission profiles to those of **Cy7**, manifesting that the sterically shielded arms on the two ortho-positions of the *meso*–aryl group do not essentially alter their ground- and excited-state conformations. Encouraged by these results, we further evaluated the chemo- and photo-stabilities of these dyes. Previous studies showed that the *meso*–phenoxy groups in the *meso* C–O aryl heptamethine indocyanines, such as **CW800** and **ZW800–1** (Scheme 1), can be rapidly exchanged by biothiol nucleophiles under aqueous conditions due to the chemically unstable *meso* C-O aryl bond [32,33]. By contrast, the *meso*–aryl heptamethine indocyanines **3a**–**3p** were considerably stable toward biothiol glutathione (GSH) due to the robust *meso* C-O aryl bond (Fig. S5 in Supporting information). In addition, previous studies also showed that the electron-rich *meso* C–O aryl or *meso* C–O alkyl heptamethine indocyanines, such as **UL766** and **CW800** (Scheme 1), are vulnerable to singlet oxygen, which results in photobleaching [36]. By comparison, the *meso*–aryl heptamethine indocyanines **3a**–**3p** even showed higher photostability than control dyes **Cy7** and **Cl-Cy7** (Fig. S6 in Supporting information), both bearing no electron-donating *meso* C–O aryl or *meso* C–O alkyl group in their molecular structures and thus being more photostable than **UL766** and **CW800**.

Having established that our "cyanine ketone method" is very convenient for constructing various robust *meso*–aryl heptamethine indocyanines, especially those anti-aggregation versions, we, as a proof-of-concept, set out to develop dye-antibody conjugate for *in vivo* imaging tumor. Indeed, monoclonal antibodies (mAb) labeled with a fluorescence reporter have shown great potentials in diagnostic applications due to their high affinity and specificity for target antigens [62]. The amine-reactive NHS ester chemistry is the most common way to fluorescently label the exposed lysine amines on mAb surface by forming an amide linkage [63,64]. Previously, we have confirmed that the small-sized *meso*–2,6-dimethoxyphenyl group could effectively prevent the self-aggregation of heptamethine indocyanine, as indicated by the exclusive monomer absorption bands of **3j** (2–40 μmol/L) in PBS (Fig. S1). Based on the consideration, we synthesized a *meso*–4–*tert*–butyl 2,6-dimethoxyphenyl **3q** from the PEGylated cyanine ketone precusor **1b** by our "cyanine ketone method" in order to install a conjugable carboxyl handle on the *meso*–2,6-dimethoxyphenyl group for protein conjugation, and the subsequent *t*–butyl deprotection by CF_3COOH provided the carboxy-functionalized congener **Tag-776** (Fig. 2A). The corresponding amine-reactive NHS ester **Tag-776-NHS**, featured with two water-soluble $(PEG)_3$ chains and an anti-aggregation *meso*–2,6-dimethoxyphenyl group, was prepared conveniently by 1-(3-dimethylaminopropyl)−3-ethylcarbodiimide (EDC) coupling. Their chemical structures were confirmed by ^{1}H NMR, ^{13}C NMR, and HRMS (Supporting information).

The photophysical properties of **Tag-776** in CH_2Cl_2, CH_3CN, and PBS (10 mmol/L, pH 7.4) were shown in Table S2 (Supporting information). As seen, **Tag-776** shows the absorption/emission maxima in the range of 762–776 nm/793–807 nm, molar extinction coefficients in the range of 2.67–3.55 × 10^5 L mol^{-1} cm^{-1}, fluorescence quantum yields in the range of 0.19–0.36, and fluorescence brightness in the range of 51,000–128,000 L mol^{-1} cm^{-1}, all of which are approximately identical to those of **3j**, indicating that the carboxyl modification does not impact its photophysical properties. Subsequently, we evaluated the water-solubility and self-aggregation of **Tag-776** in PBS (10 mmol/L, pH 7.4). As shown in Fig. 2B, due to the presence of two $(PEG)_3$ chains as well as an anti-aggregation *meso*–2,6-dimethoxyphenyl group, the dye is highly water-soluble (Lop = −0.29) and no any self-aggregation band in PBS was ob-

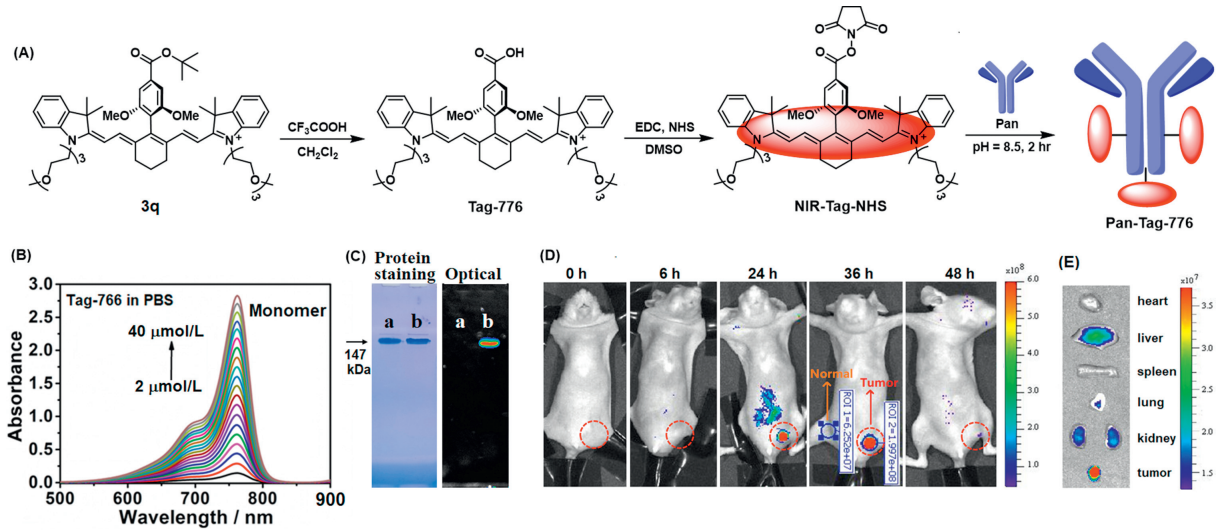

Fig. 2. (A) Synthesis of protein labeling reagent **Tag-776-NHS** and dye-antibody conjugate **Pan-Tag-776**. (B) The concentration-dependent absorption spectra of **Tag-776** (2–40 μmol/L) in pure PBS (10 mmol/L, pH 7.4). Absorption spectra were determined in 1 mm path length quartz cuvette for ensuring dyes' absorbance within the range of ultraviolet–visible (UV–vis) spectrophotometer. (C) SDS-PAGE of (a) Pan and (b) the SE-HPLC-purified **Pan-Tag-776**. Colloidal blue protein staining and optical imaging were performed after development. (D) *In vivo* fluorescence imaging of tumor using **Pan-Tag-776** (50 μg) by intravenous injection into a A549 tumor-bearing mouse *via* tail vein under a Perkinelmer *In Vivo* Imaging System. Emission was collected from **ICG** channel (λ_{ex} = 745 nm). (E) Fluorescence images of *ex vivo* biodistribution of **Pan-Tag-776** after 48 h post-injection.

served even when its concentration reached up to 40 μmol/L. Encouraged by the result, we subsequently tested whether **Tag-776** could be used to prepare dye-labeled mAb conjugate. The epidermal growth factor receptor (EGFR)-targeting mAb panitumumab (Pan) was selected for the purpose [35,45,65]. EGFR is a family of transmembrane glycoproteins, which is overexpressed in many cancer cell lines and associated with poor prognosis and high mortality [66]. To our delight, using standard protein labeling method, the corresponding NHS ester **Tag-776-NHS** could be successfully conjugated to the EGFR-targeting Pan in PBS with pH 8.5, giving rise to the dye-antibody conjugate **Pan-Tag-776** ($\lambda_{abs}/\lambda_{abs}$ = 768/800 nm in pure PBS) after purification with PD-10 column and size-exclusion column (SE-HPLC) in tandem (Fig. S7A in Supporting information). The high purity of **PAN-Tag 776** was demonstrated through sodium dodecyl sulfate-polyacrylamide gel electrophoresis (SDS-PAGE) (Fig. 2C). The degree of labeling (DOL) in the dye-antibody conjugate was determined to be ~3.0 when 10 equiv. of **Tag-776-NHS** was used (Fig. S7B in Supporting information). Animal experiment was carried out in accordance with the relevant laws and guidelines issued by the Ethical Committee of Shanxi University (No. SXULL2024010). Then, **Pan-Tag-776** (50 μg) was intravenously injected into a BALB/c nude mouse bearing A549 tumor, and imaging was carried out at 6, 24, 32, and 48 h post-injection. As shown in Fig. 2D, **Pan-Tag-776** exhibited obvious tumor uptake at the time point of 24 h, and reached up to the maximum at the time point of 32 h post-injection with a high T/N tissue ratio of 3.2, higher than the clinically acceptable threshold of 2.0. After 48 h post-injection, the fluorescence in tumor site was almost unobservable. The tumor and major organs, including heart, liver, spleen, lung, and kidney, were then removed and imaged. As shown in Fig. 2E, the residual fluorescence in liver and kidney indicates that **Pan-Tag-776** underwent both hepatic and renal clearance. These results reveal that **Pan-Tag-776** is a promising probe for the fluorescence-guided resection of tumors.

In summary, we herein have presented a new synthetic method, *i.e.*, "cyanine ketone method", for fabricating the robust *meso*–aryl heptamethine indocyanine dyes in one-pot. Using the method, various aromatic substituents, including those hydrophilic and sterically shielded ones, could be facilely installed into the *meso*–position of heptamethine indocyanines. The as-prepared water-soluble and sterically shielded *meso*–aryl heptamethine indocyanines display strong anti-aggregation abilities in water, thus facilitating their application in labeling biomacromolecules. As a proof-of-concept, we have developed a PEGylated protein labeling agent **Tag-776-NHS** for labeling monoclonal antibody Panitumumab for *in vivo* imaging tumor and achieved a high tumor-to-normal tissue ratios of 3.2. Overall, our studies lay a chemical foundation for facilely accessing the robust *meso*–aryl heptamethine indocyanine NIR fluorophores and will thus facilitate various advanced imaging and therapeutic applications.

Declaration of competing interest

The authors declare that they have no known competing financial interests or personal relationships that could have appeared to influence the work reported in this paper.

CRediT authorship contribution statement

Mengxing Liu: Software, Methodology, Investigation, Data curation. **Jing Liu:** Writing – original draft, Supervision, Resources, Project administration, Methodology, Funding acquisition, Conceptualization. **Hongxing Zhang:** Visualization, Validation, Software, Methodology, Data curation. **Jianan Tao:** Investigation, Data curation. **Peiwen Fan:** Software, Investigation. **Xin Lv:** Visualization, Validation. **Wei Guo:** Writing – review & editing, Supervision, Resources, Project administration, Funding acquisition, Formal analysis, Data curation, Conceptualization.

Acknowledgments

This work was supported by National Natural Science Foundation of China (Nos. 22277070, 22274091, 22007061), Youth Talent Support Program of Shanxi Province, Program for the Top Young Academic Leaders of Higher Learning Institutions of Shanxi, and Fundamental Research Program of Shanxi Province (No. 20210302123445).

Supplementary materials

Supplementary material associated with this article can be found, in the online version, at doi:10.1016/j.cclet.2024.109994.

References

[1] M.S.T. Gonçalves, Chem. Rev. 109 (2009) 190–212.
[2] X. Li, X. Gao, W. Shi, et al., Chem. Rev. 114 (2014) 590–659.
[3] H. Li, D. Kim, Q. Yao, et al., Angew. Chem. Int. Ed. 60 (2021) 17268–17289.
[4] R. Strack, Nat. Methods 18 (2021) 30.
[5] Z. Zeng, S.S. Liew, X. Wei, et al., Angew. Chem. Int. Ed. 60 (2021) 26454–26475.
[6] S.W. Paddock, Biotechniques 27 (1999) 992–996.
[7] H.M. Kim, B.R. Cho, Chem. Rev. 115 (2015) 5014–5055.
[8] L. Möckl, W.E. Moerner, J. Am. Chem. Soc. 142 (2020) 17828–17844.
[9] S.L. Troyan, V. Kianzad, S.L. Gibbs-Strauss, et al., Ann. Surg. Oncol. 16 (2009) 2943–2952.
[10] F. Zhang, B.Z. Tang, Chem. Sci. 12 (2021) 3377–3378.
[11] Z. Guo, S. Park, J. Yoon, I. Shin, Chem. Soc. Rev. 43 (2014) 16–29.
[12] J.L. Bricks, A.D. Kachkovskii, Y.L. Slominskii, A.O. Gerasov, S.V. Popov, Dyes Pigm. 121 (2015) 238–255.
[13] J.T. Alander, I. Kaartinen, A. Laakso, et al., Int. J. Biomed. Imaging 2012 (2012) 940585.
[14] A.P. Gorka, R.R. Nani, M.J. Schnermann, Acc. Chem. Res. 51 (2018) 3226–3235.
[15] A.P. Gorka, R.R. Nani, M.J. Schnermann, Org. Biomol. Chem. 13 (2015) 7584–7598.
[16] L. Strekowski, M. Lipowska, G. Patonay, J. Org. Chem. 57 (1992) 4578–4580.
[17] X. Ma, M. Laramie, M. Henary, Med. Chem. Lett. 28 (2018) 509–514.
[18] R.R. Nani, A.P. Gorka, T. Nagaya, et al., ACS Cent. Sci. 3 (2017) 329–337.
[19] A.P. Gorka, R.R. Nani, J. Zhu, S. Mackem, M.J. Schnermann, J. Am. Chem. Soc. 136 (2014) 14153–14159.
[20] S.M. Usama, S. Thavornpradit, K. Burgess, ACS Appl. Bio Mater. 1 (2018) 1195–1205.
[21] L. Jiao, F. Song, J. Cui, X. Peng, Chem. Commun. 54 (2018) 9198–9201.
[22] S. Luo, X. Tan, S. Fang, et al., Adv. Funct. Mater. 26 (2016) 2826–2835.
[23] X. Zhao, H. Zhao, S. Wang, et al., J. Am. Chem. Soc. 143 (2021) 20828–20836.
[24] S. Hernot, L.V. Manen, P. Debie, et al., Lancet Oncol. 20 (2019) e354–e367.
[25] P. Debie, S. Hernot, Front. Pharmacol. 10 (2019) 510.
[26] P. Debie, J. Quathem, I. Hansen, et al., Mol. Pharm. 14 (2017) 1145–1153.
[27] C. Cilliers, I. Nessler, N. Christodolu, G.M. Thurber, Mol. Pharm. 14 (2017) 1623–1633.
[28] E.A. Owens, M. Henary, G. El Fakhri, H.S. Choi, Acc. Chem. Res. 49 (2016) 1731–1740.
[29] H. Hyun, M. Henary, T. Gao, et al., Mol. Imaging Biol. 18 (2016) 52–61.
[30] H.S. Choi, L. Narayana, M. Henary, et al., J. Med. Chem. 58 (2015) 2845–2854.
[31] H.S. Choi, S.L. Gibbs, J.H. Lee, et al., Nat. Biotechnol. 31 (2013) 148–153.
[32] S.Y. Lim, K.H. Hong, D.I. Kim, H. Kwon, H.J. Kim, J. Am. Chem. Soc. 136 (2014) 7018–7025.
[33] A. Zaheer, T.E. Wheat, J.V. Frangioni, Mol. Imaging 1 (2002) 354–364.
[34] J. Cha, R.R. Nani, M.P. Luciano, et al., Bioorg. Med. Chem. Lett. 28 (2018) 2741–2745.
[35] K. Sato, A.P. Gorka, T. Nagaya, et al., Bioconjug. Chem. 27 (2016) 404–413.
[36] M.P. Luciano, S.N. Crooke, S. Nourian, et al., ACS Chem. Biol. 14 (2014) 934–940.
[37] D. Su, C.L. Teoh, A. Samanta, et al., Chem. Commun. 51 (2015) 3989–3992.
[38] Z. Wu, P. Shao, S. Zhang, M. Bai, J. Biomed. Opt. 19 (2014) 036006.
[39] H. Lee, J.C. Mason, S. Achilefu, J. Org. Chem. 71 (2006) 7862–7865.
[40] S. van der Wal, J. Kuil, A.R.P.M. Valentijn, F.W.B. van Leeuwen, Dyes Pigm. 132 (2016) 7–19.
[41] H. Hyun, E.A. Owens, L. Narayana, et al., RSC Adv. 4 (2014) 58762–58768.
[42] Y. Zhou, Y.S. Kim, D.E. Milenic, K.E. Baidoo, M.W. Brechbiel, Bioconjug. Chem. 25 (2014) 1801–1810.
[43] Y. Ji, Z. Wang, K. Bao, et al., Quant. Imaging Med. Surg. 9 (2019) 1548–1555.
[44] D.H. Li, C.L. Schreiber, B.D. Smith, Angew. Chem. Int. Ed. 59 (2020) 12154–12161.
[45] S.M. Usama, S.C. Marker, D.H. Li, et al., J. Am. Chem. Soc. 145 (2023) 14647–14659.
[46] H. Lee, J.C. Mason, S. Achilefu, J. Org. Chem. 73 (2008) 723–725.
[47] L. He, W. Lin, Q. Xu, et al., Chem. Sci. 6 (2015) 4530–4536.
[48] S.G. König, R. Krämer, Chem. Eur. J. 23 (2017) 9306–9312.
[49] J. Salon, E.A. Wolińska, A. Raszkiewicz, G. Patonay, L. Strekowski, J. Heterocycl. Chem. 42 (2005) 959–961.
[50] A. Levitz, F. Marmarchi, M. Henary, Photochem. Photobiol. Sci. 17 (2018) 1409–1416.
[51] L. Štacková, P. Štacko, P. Klán, J. Am. Chem. Soc. 141 (2019) 7155–7162.
[52] Y. Koide, Y. Urano, K. Hanaoka, T. Terai, T. Nagano, J. Am. Chem. Soc. 133 (2011) 5680–5682.
[53] X. Lv, C. Gao, T. Han, H. Shi, W. Guo, Chem. Commun. 56 (2020) 715–718.
[54] J. Liu, Y. Sun, H. Zhang, et al., ACS Appl. Mater. Interfaces 8 (2016) 22953–22962.
[55] Y. Dong, X. Lu, Y. Li, et al., Chin. Chem. Lett. 34 (2023) 108154.
[56] L. Strekowski, M. Lipowska, G. Patonay, Synth. Commun. 22 (1992) 2593–2598.
[57] L. Strekowski, J.C. Mason, H. Lee, M. Say, G. Patonay, J. Heterocyclic Chem. 41 (2004) 227–232.
[58] Y. Kim, Y. Choi, R. Weissleder, C.H. Tung, Bioorg. Med. Chem. Lett. 17 (2007) 5054–5057.
[59] Z. Guo, S. Nam, S. Park, J. Yoon, Chem. Sci. 3 (2012) 2760–2765.
[60] H. Chong, S. Wen, J. Cao, et al., Org. Lett. 15 (2013) 4022–4025.
[61] X. Wang, Z. Guo, S. Zhu, H. Tian, W. Zhu, Chem. Commun. 50 (2014) 13525–13528.
[62] J.S.D Mieog, F.B. Achterberg, A. Zlitni, et al., Nat. Rev. Clin. Oncol. 19 (2022) 9–22.
[63] G.W. Anderson, F.M. Callahan, J.E. Zimmerman, J. Am. Chem. Soc. 89 (1967) 178.
[64] O. Koniev, A. Wagner, Chem. Soc. Rev. 44 (2015) 5495–5551.
[65] Y. Liao, Y. Liang, Y. Huang, et al., Chin. Chem. Lett. 35 (2024) 109092.
[66] T. Barrett, Y. Koyama, Y. Hama, et al., Clin. Cancer Res. 13 (2007) 6639–6648.